Journal of General Virology (2004), **85**, 3367–3376 DOI 10.1099/vir.0.80203-0

Dual role of the adenovirus pVI C terminus as a nuclear localization signal and activator of the viral protease

K. S. Honkavuori, B. D. Pollard, M. S. Rodriguez,† R. T. Hay and G. D. Kemp

Biomolecular Sciences Building, University of St Andrews, North Haugh, St Andrews KY16 9ST, UK

Correspondence
G. D. Kemp
gdk@st-andrews.ac.uk

Received 18 April 2004
Accepted 6 July 2004

Adenain, the protease produced by adenovirus, is regulated by formation of a heterodimer with an 11 aa peptide derived from the C terminus of another adenoviral protein, pVI. Here, the role of the basic motif KRRR, which is conserved in pVI sequences from human adenovirus serotypes, was investigated. It was shown that this motif is less important than the N- or C-terminal regions in the formation of the adenain–peptide heterodimer and in the activity of the subsequent complex. This motif, however, acted as a nuclear localization signal that was capable of targeting heterologous proteins to the nucleus, resulting in a distinctive intranuclear distribution consisting of discrete foci, which is similar to that found for pVI during adenovirus infection.

INTRODUCTION

In common with many other viruses, adenovirus encodes its own protease and depends on its action for the development of infectivity (Anderson *et al.*, 1973; Weber, 1976). The adenovirus protease (adenain) is synthesized late in infection and packaged into the immature virus particle, where its action in cleaving at least six of the viral proteins (pVI, pVII, pVIII, protein IIIa, X and the pre-terminal protein) results in the formation of the mature, infectious virion (Anderson *et al.*, 1973; Boudin *et al.*, 1980; Tremblay *et al.*, 1983). Adenain is also known to be active in the cytoplasm where it has been shown to cleave cytokeratins, an action that may be important in facilitating release of the virus from the cell (Chen *et al.*, 1993). It has also been reported that adenain is active at different times and in different locations within the adenovirus infectious cycle (Greber, 1998); thus, knowledge of the mechanisms involved in its regulation and localization is essential in understanding the process of adenovirus infection.

One distinctive characteristic of adenain is that its activity is regulated by the formation of a disulphide-linked heterodimer with an 11 aa peptide (GVQSLKRRRCF) derived from the C terminus of another adenoviral protein, pVI, and termed pVI-CT (Mangel *et al.*, 1993; Webster *et al.*, 1993). It has been suggested that the disulphide-linked pVI-CT–adenain dimer is required for activation and that a form of thiol–disulphide interchange results in formation of the active heterodimer, involving C104 of adenain (Webster *et al.*, 1993).

†Present address: Institut Jacques Monod, CNRS, Tour 43–44, 2 Place Jussieu, 75005 Paris, France.

Ding *et al.* (1996) described adenain as an ovoid structure with two mini-domains, one characterized by a four-stranded sheet and the other containing three major α-helices. The active-site histidine (H54) lies at the end of one of the β-strands, whilst the nucleophilic cysteine (C122) is part of one of the α-helices. G1 and V2 of pVI-CT fit into a pocket that is formed between two of the major α-helices, whereas aa 4–10 form an additional strand to the β-sheet, indicating that activation may be a result of 'tying together' the two mini-domains and creating and stabilizing the active conformation (Cabrita *et al.*, 1997).

Recently, Wodrich *et al.* (2003) drew attention to the fact that pVI contains two nuclear export signals (NESs) and two nuclear localization signals (NLSs). One NLS is located in pVI-CT and one NES straddles the boundary between pVI-CT and the remainder of pVI (iVI). These authors demonstrated that pVI is capable of transporting the adenovirus hexon protein to the nucleus and further suggested that, as part of that role, pVI is capable of shuttling between the cytoplasm and the nucleus.

Alignment of the pVI-CT sequences from human adenoviruses shows that aa 6–9 are completely conserved in a distinctive basic motif, KRRR (Fig. 1). The aim of the work described here was to determine the influence of this motif on the function of the adenain system. The data presented show that these residues are much less important than G1, V2, C10 and F11 in the binding of pVI-CT to the protease and for the activity of the heterodimer. These findings are in accord with those of Baniecki *et al.* (2001), which were obtained by using a different binding assay. This motif does, however, constitute one of two potential NLSs in pVI that were reported by Wodrich *et al.* (2003). The data

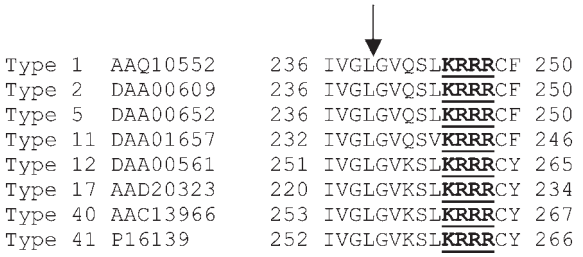

Fig. 1. Sequence alignment of C-terminal residues of human adenovirus pVI proteins. The protease cleavage site is indicated by an arrow, whilst conserved cationic residues are underlined and in bold. Sequences (accession nos shown) were derived from the NCBI and SWISS-PROT protein databases and aligned by using the CLUSTAL sequence-alignment program at EMBL/EBI (European Bioinformatics Institute).

presented here confirm and extend the observations of Wodrich *et al.* (2003) by defining the minimum sequence that is necessary by mutational analysis. We also demonstrated that, whilst both NLSs were required for nuclear localization of pVI, the KRRR motif was capable of targeting other proteins to the nucleus on its own. Furthermore, it caused an intranuclear distribution into distinct foci, which is characteristic of the pVI distribution that is observed during adenovirus infection. We have also reported the use of this motif in the construction of fluorescent substrates for adenain that are capable of demonstrating the appearance of adenain activity in the cell nucleus following infection.

METHODS

Peptides were synthesized by the fluorenylmethoxycarbonyl polyamide method of Atherton *et al.* (1988) and purified by reverse-phase chromatography on a C18 column that was pre-equilibrated with 0·1 % (v/v) trifluoroacetic acid as described previously (Webster *et al.*, 1989). Peptides were eluted with increasing concentrations of acetonitrile. Peptides were verified by matrix-assisted laser desorption/ionization mass spectrometry (TofSpec 2; Micromass) and by N-terminal sequencing (Procise; Applied Biosystems).

Expression and purification of adenain. Adenain was expressed in and purified from *Escherichia coli* BL21(DE3) as described previously (Anderson, 1990; Grierson *et al.*, 1994). Protein and peptide concentrations were determined as described previously (Cabrita *et al.*, 1997).

Non-denaturing, non-reducing, 'native' gel electrophoresis. The 'native' gel electrophoresis for basic proteins was a method adapted from that of Goldenberg (1989). To obtain 'native' conditions for adenain and pVI-CT binding, riboflavin was used with tetramethylethylenediamine for photopolymerization in the absence of SDS. In a typical binding assay, 4 µl containing 400 ng adenain and 500 ng lysozyme in 50 mM Tris/HCl (pH 8) was mixed with 5 µl of varying concentrations (1 mM to 4 µM in 50 mM Tris/HCl, pH 8) of pVI-CT or its variants and 12·5 µl 50 mM Tris/HCl, 10 mM EDTA, 2 mM 2-mercaptoethanol. After 5 min at room temperature, samples were mixed with 10 µl 0·8 % methyl green, 20 % glycerol; 20 µl from each mixture was applied to a 15·4 % (w/v) polyacrylamide gel. Following electrophoresis for 40 min at 180 V, gels were stained and destained as described previously (Webster *et al.*, 1993). Gels were scanned by using a Canoscan FB 636U scanner and densitometric analysis of the bands was performed by using the public domain NIH Image program (developed at the US National Institutes of Health; http://rsb.info.nih.gov/nih-image/).

In the absence of activating peptide, adenain migrates as a diffuse band; the presence of lysozyme was used to normalize total adenain concentration. In all gels, one reference lane contained wild-type pVI-CT in a 300-fold molar excess over adenain. Under these conditions, all of the adenain is found in the heterodimer. The proportion of adenain complexed with activating peptide (and thus the amount of bound activating peptide) in the other lanes was determined by comparison with this reference lane. This process assumes that adenain and pVI-CT form a 1 : 1 complex, as indicated by the structural studies of Ding *et al.* (1996).

Activity assays. The K_m and k_{cat} values for protease and peptide mutants were obtained from activity assays with the fluorogenic substrate z-Leu-Arg-Gly-Gly-AMC (z-LRGG-AMC; Bachem). Activity assays were performed in assay buffer (50 mM Tris/HCl, 10 mM EDTA, pH 8, with 2 mM 2-mercaptoethanol) with 26 nM adenain and 2 µM peptide. The assay mixtures were pre-incubated at 37 °C for 5 min before the addition of the fluorogenic substrate from a 50 mM stock solution in DMSO. Increase in fluorescence was measured by using a Perkin-Elmer LSB50 luminescence spectrometer at excitation wavelength 370 nm and emission wavelength 460 nm. Each experiment was performed in triplicate. In order to determine k_{cat} values, the concentration of activated protease was calculated as described by Baniecki *et al.* (2001) from K_d values obtained by native gel electrophoresis.

In experiments to determine K_d from the kinetic constants, 26 nM purified adenain and varying concentrations of peptide (0·3–3 µM) were incubated in assay buffer prior to the addition of 62·5 µM substrate. Assays were performed at 37 °C. For K_m and k_{cat} determinations, the peptide concentration was kept at 2 µM and the substrate concentration was altered from 15·6 to 200 µM. Otherwise, the experiments to determine K_d by this approach were conducted in an identical manner to the determination of K_m and k_{cat}.

Cell culture, transfections and infections. HeLa cells were used in transient transfections and infections by human adenovirus type 2 (Ad2). The cells were maintained at 37 °C in 5 % CO_2 in Dulbecco's modified Eagle's medium (Gibco) supplemented with 10 % fetal calf serum (Gibco). Cells were transfected by using FuGene transfection reagent (Roche) according to the manufacturer's instructions. Cells were fixed 16–24 h after initial transfection with 3 % paraformaldehyde in PBS. For microscopy, cells were grown on glass cover slips, which were mounted on to slides with 90 % glycerol/10 % PBS containing DAPI. For the pyruvate kinase (PK) constructs, 9E10CD antibody, which is specific for PK (a gift from C. Dargement, Institut Curie-CNRS, Paris), was used, together with secondary antibody conjugated to fluorescein isothiocyanate (FITC; Oxford Biotechnology). For the labelling of pVI/iVI/VI in infected cells, a rabbit polyclonal anti-pVI antibody, raised against aa 94–170 of pVI of Ad2, was used (a gift from W. C. Russell, University of St Andrews, UK), together with FITC-conjugated anti-rabbit Ig.

Virus propagation. The preparation and purification of Ad2 was performed as described by Russell & Blair (1977). Viral infections were performed at an m.o.i. of 5–10.

Fluorescence microscopy. Fluorescent images were acquired by using a DeltaVision restoration microscope (Applied Precision) and analysed by using *softWoRx* software. Indirect immunofluorescence was performed as reported previously (Rodriguez *et al.*, 2001). Images were acquired by using a Nikon Microphot-FXA microscope and a 100× oil-immersion lens.

Cytoplasmic and nuclear fractionation of transfected cells. To obtain separate cytoplasmic and nuclear extracts from transfected cells, cells grown on six-well plates were transfected by using FuGene. At 24 h after initial transfection, cells were removed by using a cell scraper and resuspended in 200 µl 10 mM HEPES (pH 8), 50 mM NaCl, 0·5 M sucrose, 1 mM EDTA, 0·5 mM spermidine, 0·15 mM spermine and 0·2 % Triton X-100. The lysate was left on ice for 6 min and centrifuged at 6500 r.p.m. by using a Sigma 3K10 centrifugator for 3 min at 4 °C. The resulting supernatant was stored at −70 °C as the cytoplasmic fraction. The pellet was washed with 200 µl 50 mM NaCl, 10 mM HEPES, 25 % glycerol, 0·1 mM EDTA, 0·5 mM spermidine, 0·15 mM spermine and centrifuged at 6500 r.p.m. for 3 min at 4 °C, after which the supernatant was discarded. The pellet was resuspended carefully in 100 µl 350 mM NaCl, 10 mM HEPES, 25 % glycerol, 0·1 mM EDTA, 0·5 mM spermidine and 0·15 mM spermine and left on ice for 30 min with regular mixing. The lysate was centrifuged at 6500 r.p.m. for 20 min at 4 °C and the supernatant was stored at −70 °C as the nuclear extract until further analysis. All buffers contained a cocktail of protease inhibitors (Roche), added immediately before use.

SDS-PAGE and Western blotting. The nuclear and cytoplasmic fractions were subject to 15 % SDS-PAGE followed by transfer to nitrocellulose membrane by Western blotting, as described previously (Grierson *et al.*, 1994). To detect expression of pVI–EGFP and mutants (see below), a rabbit anti-GFP antibody (Roche) was used.

Plasmid construction. For all plasmid constructs, the oligonucleotides for PCR were purchased from Oswel DNA Services. The constructs generated were sequenced at the University of St Andrews DNA sequencing unit. Vent DNA polymerase (New England Biolabs) was used for the PCRs, which were conducted according to the manufacturer's instructions.

Construction of pVI and mutants in pEGFP-C1. pVI cDNA was amplified by PCR from Ad2 and the PCR-generated mutants were inserted at the C terminus of the pEGFP-C1 and pDsRED2-C1 (containing red fluorescent protein) plasmids (Clontech), using the *Eco*RI/*Bam*HI restriction sites (underlined below). The oligonucleotides used for amplification of the C-terminal mutant of pVI–EGFP (mutation of KRRR to four alanines) were (1) 5′- GCTCAAGCTTCGAATTCC**ATGGAAGAC**-3′ (N terminus of pVI is shown in bold) and (2) 5′-CGGTGGATCCTTAGAAGCA**TGCTGCGGCCGC**-CAGGGATTGCAC-3′ (introduced mutations are shown in bold). To obtain the middle mutant (MM) of pVI–EGFP, the KRPRP sequence was mutated to five alanines by using oligonucleotide (1) together with oligonucleotide (3) (5′-CCTGTC**GGCCGCCGCC-GCCGC**TTCGCCACGCCC-3′). The resulting fragment was used together with the C-terminal pVI–EGFP oligonucleotide (4) (5′-CGGTGGATCCTTAGAAGCATCGTCG-3′) for a second PCR to obtain the full-length insert. The double mutant (DM) of pVI was obtained by using the MM as a template for the PCR with oligonucleotides (1) and (2). Truncated forms of pVI were synthesized as follows. The 34–250 aa truncated pVI protein was generated by using oligonucleotide (4) together with oligonucleotide (5) (5′-GCTTCGAATTCTGCCTTCAGCTGGGGCTCG-3′). Similarly, the intermediate form of pVI (iVI; aa 1–239) was generated by using oligonucleotides (1) and (6) (5′-GGAGGATCCTTACAGACCCA-CGATGCTG-3′). The mature VI (aa 34–239) was synthesized by combining oligonucleotides (5) and (6).

Construction of PK fusion proteins. The KRRR sequence and single alanine mutants thereof were expressed in plasmid pcDNA-PK. Synthetic complementary oligonucleotides were annealed and cloned into the *Bam*HI/*Xba*I sites at the C terminus of PK. The sequences of the sense oligonucleotides [restriction sites underlined, mutation(s) in bold] were: PKKKRKV (SV40 large T antigen NLS), 5′-GATCCGCTCCAAAGAAGAAGCGCAAGGTGGAATAGT-3′; KRRRCF, 5′-GATCCTCTCTTAAACGTCGTCGTTGTTTTTAGG-3′; K**ARA**CF, 5′-GATCCTCTCTTAAA**GCT**CGT**GCT**TGTTTTTAGT-3′; **AARA**CF, 5′-GATCCTCTCTT**GCTGCT**CGT**GCT**TGTTTTTAGT-3′; **A**RRRCF, 5′-GATCCTCTCTT**GCT**CGTCGTCGTTGTTTTTAGT-3′; K**A**RRCF, 5′-GATCCTCTCTTAAA**GCT**CGTCGTTGTTTTTAGG-3′; KR**A**RCF, 5′-GATCCTCTCTTAAACGT**GCT**CGTTGTTTTTAGG-3′; KRR**A**CF, 5′-GATCCTCTCTTAAACGTCGT**GCT**TGTTTTTAGG-3′.

Construction of fluorescent substrates based on pVI. Substrates containing pVI or its derivatives fused to the enhanced yellow fluorescent protein (EYFP) and enhanced cyan fluorescent protein (ECFP) were prepared as follows. The pcDNA 3.1-based plasmid pdf20 (a gift from P. de Felipe, University of St Andrews, UK) was used as a template for the constructs 20.1–20.6. The plasmid pdf20, containing the cytomegalovirus promoter, contained EYFP–2A–ECFP–2A–Pac inserts (2A, picornavirus 2A protein; Pac, puromycin-*N*-acetyltransferase). ECFP and EYFP sequences were from Clontech. In this study, 2A–ECFP–2A inserts were removed by *Xba*I/*Apa*I digestion followed by insertion of the pVI sequence or C-terminal fragments of it, by using the above restriction sites. To obtain constructs 20.2, 20.4 and 20.6, the ECFP–2A fragment was inserted back into the C terminus of the pVI sequence in constructs 20.1, 20.3 and 20.5 by using the *Apa*I site. The following primers were used for PCRs: 5′-CAAAAGGGCCC*ACCGCCAGC*GGCCGC-**GAAGCATCGTCGGCGCTTCAGGGA**-3′ (pVI C-terminal primer for all constructs); 5′-GAAAATCTAGA*GGTGGCGGA*GAATTC-**GGTCCGCGATCGATGCGGCCCGTAGCC**-3′ (for construct 20.1: 34 aa from the C terminus of pVI); 5′-GAAAATCTAGA*GGTGG-CGGA*GAATTC**GTGCTGGGCCAGCACACACCTGTAACG**-3′ (for construct 20.3: 79 aa from the C terminus of pVI); and 5′-GAAAATCTAGA*GGTGGCGGA*GAATTC**ATGGAAGACATCAACT-TTGCGTCTCTGG** (for construct 20.5, full-length pVI). *Apa*I/*Xba*I restriction sites in the oligonucleotides are underlined and sequences from pVI are shown in bold. The glycine residues (in italics) were inserted to allow flexibility between the fluorescent proteins and the pVI inserts.

RESULTS

pVI-CT binding of adenain: the terminal residues of pVI-CT are of most significance

Previous work (Jones *et al.*, 1996) has shown that binding of pVI-CT to adenain results in a conformational change in adenain that alters its intrinsic tryptophan fluorescence. These authors further demonstrated that this conformational change did not occur when using pVI-CT variants that lacked the N-terminal G and V residues, nor with a variant where C10 was replaced by A. The importance of these residues was further confirmed by data that showed that the desGV (missing the G and V residues) and C10A variants were much less effective than wild-type pVI-CT in activating adenain (Cabrita *et al.*, 1997).

Alignment of pVI-CT sequences from human adenovirus serotypes (Fig. 1) showed that these residues were well-conserved, but that there was also conservation of a distinctive 4 aa basic motif (KRRR) occupying positions 6–9. The importance of these residues was investigated by using a technique based on gel electrophoresis under non-denaturing conditions (native gel electrophoresis). In the

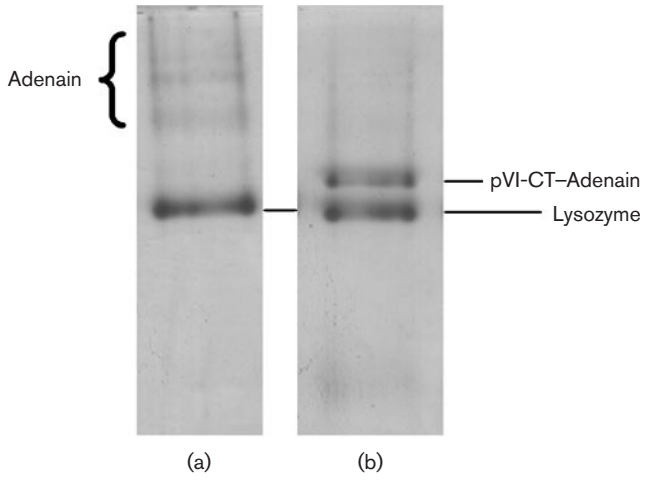

Fig. 2. Native gel electrophoresis of adenain and adenain–pVI-CT. Adenain (11·6 pmol) separated by non-reducing, non-denaturing gel electrophoresis in the absence (a) and presence (b) of a 300-fold molar excess of pVI-CT. Adenain solutions contained equimolar amounts of lysozyme as an internal standard.

absence of SDS or mercaptoethanol, adenain does not migrate as a distinct band, but rather as a diffuse smear. However, this changes in the presence of pVI-CT and quantification of the distinct band of the protein–peptide heterodimer provided a measure of the concentration of bound pVI-CT and allowed the determination of binding constants (Fig. 2).

The K_d values for complexes between adenain and wild-type pVI-CT and alanine variants of residues K6, R7, R8, R9 and F11 are shown in Table 1. F11A was the only variant that showed any significant alteration in binding affinity ($P<0{\cdot}001$), with a value more than four times higher than that of wild-type pVI-CT. A similar pattern was evident in the values of K_m and k_{cat}, derived from experiments where adenain was activated by different variants of pVI-CT. Substitution of alanine into the basic motif had little effect, whereas the complex involving the F11A variant has its K_m value increased fourfold and there was a 3·8-fold reduction in k_{cat}.

The observation that none of the residues in the well-conserved KRRR motif had an important role in the formation or subsequent catalytic activity of the pVI-CT–adenain complex suggested that they have another role. We therefore investigated the possibility that they acted as an NLS.

The KRRR motif can act as an NLS

To establish whether the KRRR motif could function as an NLS, the wild-type sequence and single alanine mutants thereof were assayed for their ability to confer nuclear accumulation of an otherwise cytoplasmic protein, Myc-tagged PK. The SV40 large T antigen has one of the best-characterized NLSs, the PKKKRKV sequence (Kalderon *et al.*, 1984) and in this study, this sequence, which is capable of directing a cytoplasmic protein to the nucleus, was used as a positive control. For immunofluorescence, the generated PK fusion proteins were detected by using an anti-Myc antibody (9E10).

As illustrated in Fig. 3, in addition to the PK–SV40 NLS construct, the PK KRRR construct (the C terminus of pVI-CT) was sufficient to confer nuclear accumulation. PK KRRA and KRAR constructs were also detected in the nucleus, albeit to a lesser extent, especially in the case of KRAR. This sequence has previously been described as an NLS for adenovirus fibre protein. However, in the case of adenovirus fibre experiments, KRAR was also unable to target *E. coli* β-galactosidase, a cytoplasmic protein, solely to the nucleus (Hong & Engler, 1991).

In addition to the PK control (no NLS), the PK constructs KARR, ARRR, KARA and AARA were cytoplasmic. Therefore, in this study, the minimal signal sequence requirement for the nuclear localization of PK was the cationic

Table 1. Binding constants and kinetic data for adenain and pVI-CT variants

Values for the dissociation constant (K_d) were determined by native gel electrophoresis. Values determined by the method of Baniecki *et al.* (2001) from activity assays using the substrate z-LRGG-AMC are shown in parentheses. In the calculation of k_{cat}, the K_d values assessed by native gel electrophoresis were used to determine the concentration of the active peptide–protease heterodimer. Values given are replicates of at least three separate experiments.

Peptide	K_d (μM)	K_m (μM)	k_{cat} (s^{-1})
GVQSLKRRRCF	1·28 ± 0·19 (1·62 ± 0·16)	49·1 ± 16·5	0·0283 ± 0·004
GVQSL**A**RRRCF	2·82 ± 1·51 (2·5 ± 0·4)	135 ± 44·4	0·0202 ± 0·0038
GVQSLK**A**RRCF	1·45 ± 0·12 (1·34 ± 0·39)	98·55 ± 15·5	0·017 ± 0·0014
GVQSLKR**A**RCF	1·55 ± 0·30 (2·19 ± 0·18)	61·6 ± 21	0·0161 ± 0·0024
GVQSLKRR**A**CF	1·47 ± 0·27 (1·01 ± 0·30)	60·9 ± 12·7	0·0173 ± 0·0016
GVQSLKRRRC**A**	5·88 ± 0·28 (7·46 ± 1·64)	200 ± 92·9	0·0075 ± 0·0022

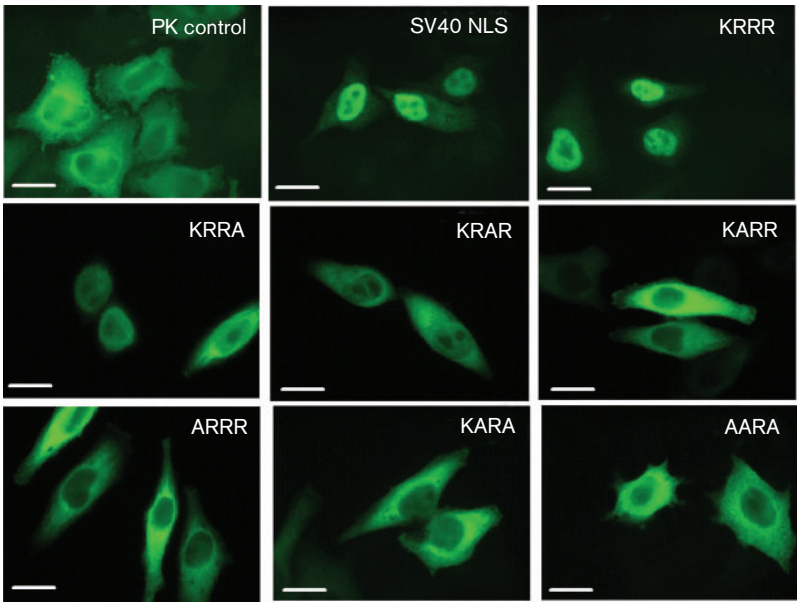

Fig. 3. Localization of PK and peptide sequence fusions. HeLa cells were transfected with plasmids expressing PK (PK control), PK fused to the known NLS from SV40 (SV40 NLS) or PK fused to the tetrapeptides indicated. The localization of PK or its fusion products was determined by immunofluorescence using an antibody to PK after fixation of the cells. Bars, 10 μm.

tripeptide KRR. These data are in accord with the observations of Wodrich *et al.* (2003), who showed that the C terminus of pVI makes an important contribution to the ability of pVI to transport the adenovirus hexon protein to the nucleus.

Role of the KRRR motif in localization of pVI

The adenovirus pVI sequence contains two putative NLSs. In addition to the KRRR motif at aa 245–248, close to the C terminus of this 250 aa protein, another potential NLS is situated in the middle of the protein, namely the KRPRP motif at aa 131–135. This motif is conserved in the pVI sequences from other human serotypes and is also found in the adenovirus E1a protein, and has been proposed to act as an NLS (Lyons *et al.*, 1987).

To assess the relative importance of the KRPRP and KRRR sequences for the nuclear accumulation of pVI, they were mutated individually to alanine residues to obtain MM and C-terminal mutants (CM), respectively. Both putative signal sequences were abolished to obtain the DM. These mutants were cloned and expressed in fluorescent vectors pEGFP-C1 and pDsRED2-C1. In addition, truncated forms of pVI, corresponding to aa 34–250, 1–239 and 34–239, were generated. Two of these mimic the natural cleavage products of adenain, 1–239 being the intermediate iVI and 34–239 being the mature VI. The localization of these was assessed by fluorescence microscopy and Western blotting analysis of nuclear and cytoplasmic fractions of transfected HeLa cells at 24 h after initial transfection.

Söling *et al.* (2002) found that the fluorescent protein tag affected the nuclear localization of herpes simplex virus type 1 thymidine kinase. In our study, the pVI protein and its mutants localized in an identical manner, whether expressed as a fusion with EGFP or DsRED2 fluorescent protein (EGFP images only are presented here).

As seen in Fig. 4(a), the CM and MM mutants were found in both the cytoplasm and the nucleus with a punctate distribution. The DM, however, was mainly found in the cytoplasm. None of the mutants was capable of complete nuclear accumulation similar to that observed with the wild-type pVI protein. The synthesized truncated proteins 1–239 (iVI) and 34–239 (VI) localized similarly, having both lost one of their NLSs. The deletion mutant 34–250 was also incapable of complete nuclear accumulation, despite possessing both putative NLSs. This was presumably due to a conformational change in the structure of the protein after deletion of the first 33 aa or may indicate the presence of a nuclear retention signal in this section of the protein.

Western blot analysis of nuclear and cytoplasmic fractions confirmed that most of the deletion mutants and NLS mutants were present in both fractions (Fig. 4b), in comparison with the wild-type pVI, which was solely nuclear. Overall, the results suggested that the KRPRP and KRRR motifs are both required for nuclear accumulation of the pVI protein, although the KRRR motif on its own is capable of directing a heterologous protein to the nucleus.

To assess further the efficacy of the KRRR motif as an NLS for other proteins, we constructed plasmids containing sequences of different lengths from the C terminus of pVI, as well as the full-length pVI, between two fluorescent proteins, EYFP and ECFP, or between EYFP and the puromycin resistance-encoding gene (*pac*) (Table 2). The EYFP and EYFP–ECFP plasmids were constructed from plasmid pdf20 and used for transient transfections of HeLa cells by using FuGene. The localization of the plasmid

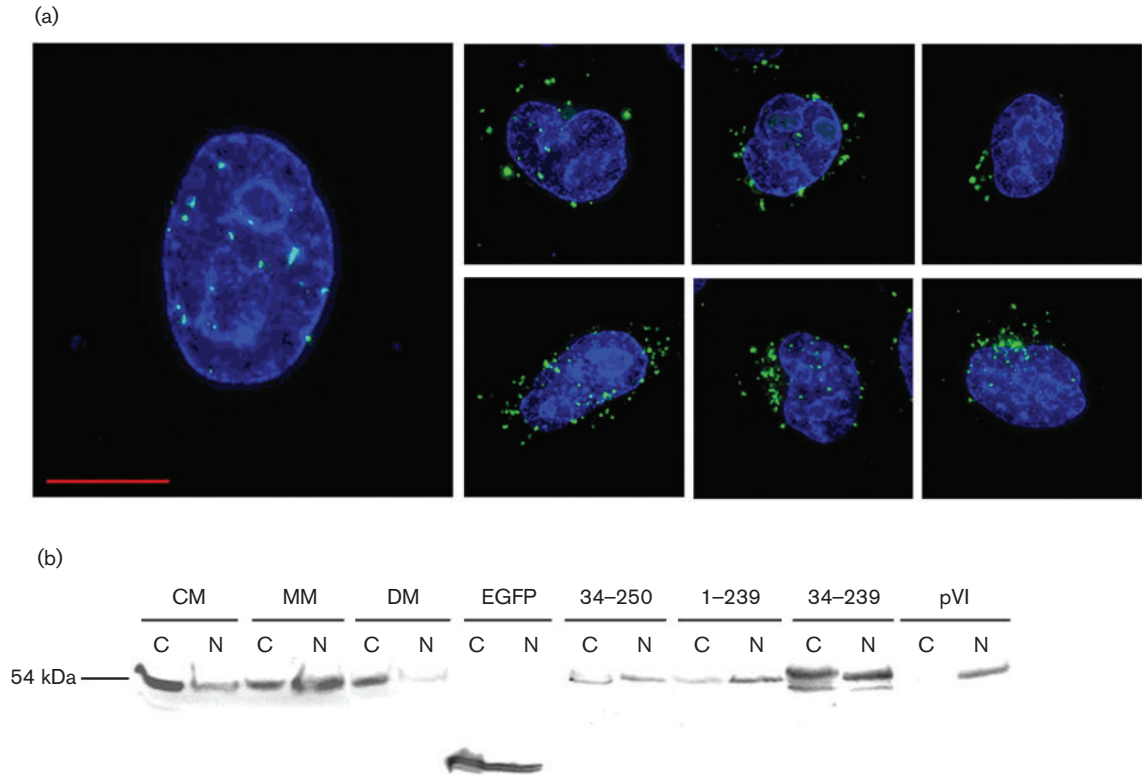

Fig. 4. Importance of the two putative NLSs for the localization of pVI. (a) HeLa cells were transfected with plasmids expressing EGFP fused to wild-type pVI (pVI–EGFP); mutants of pVI with alanine residues replacing the residues encoding the C-terminal NLS (CM), the mid-sequence NLS (MM) and both NLSs (DM); and truncated forms of pVI comprising aa 34–250, 1–239 and 34–239. EGFP fusions were detected directly by fluorescence microscopy after fixation of cells. Bar, 10 μm. (b) Western blot analysis of cytoplasmic (C) and nuclear (N) extracts following transfection with plasmids expressing EGFP alone (EGFP) or EGFP fused to wild-type pVI (pVI); mutants of pVI with alanine residues replacing the residues encoding the C-terminal NLS (CM), the mid-sequence NLS (MM) or both NLSs (DM); and truncated forms of pVI comprising aa 34–250, 1–239 or 34–239. Proteins were detected by using a rabbit anti-GFP antibody.

constructs 20 (control) and 20.1–20.6 was followed by using a DeltaVision restoration microscope. Successful nuclear accumulation was evident for all EYFP and EYFP–ECFP constructs with the exception of 20.2 (Fig. 5). Construct 20.2, containing 34 aa from the C terminus of pVI, was found throughout the cytoplasm and nucleus. The most likely explanation for this, especially as construct 20.1 accumulated in the nucleus, is that the signal sequence is buried in between the two fluorescent proteins and is thus inaccessible. Thus, whilst the Pac protein does not hinder recognition of the NLS in the case of construct 20.1, ECFP, presumably due to its size, does. This is in accord with reports that the karyophilic domain needs to be exposed on the surface of the protein to function as an NLS (Roberts *et al.*, 1987).

Following transfection, the pVI fusion proteins that localized in the nucleus displayed a distinctive punctate pattern (Fig. 5), although overexpression led to diffuse nuclear fluorescence with time. To address the possibility that this might be an artefact or might be influenced by the presence of the fusion partner, HeLa cells were infected with adenovirus and the distribution of pVI and derivatives was determined 22 h after infection by using an antibody raised against pVI. As shown in Fig. 5(h), an identical punctate pattern, apparently avoiding the nucleolus, was evident in infected cells.

Fluorescent constructs enable the *in vivo* detection of adenain activity during infection

As well as containing the putative NLS, constructs 20.2 and 20.4 also contained an adenain cleavage site, whilst construct 20.6 contained two such sites. As these cleavage sites lay between two proteins with different fluorescent properties, these constructs had the potential to act as substrates that could be used to localize protease activity during infection. To determine whether the fusions could be cleaved by adenain, a rabbit reticulocyte lysate transcription–translation system (Promega) was primed with constructs 20.1–20.6 and the expressed protein was incubated with purified recombinant adenain and pVI-CT.

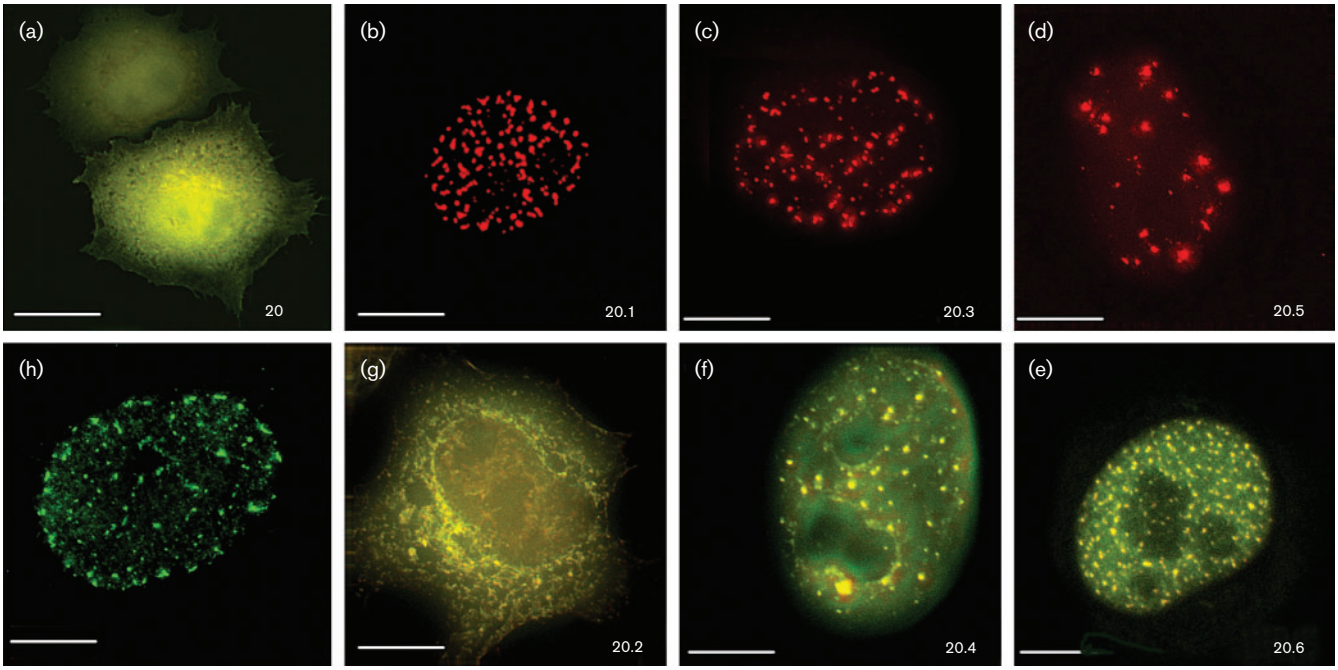

Fig. 5. Subcellular localization of fluorescently tagged pVI and derivatives. HeLa cells were transfected with plasmids containing construct 20 (a) and constructs 20.1–20.6 (b–g). Fusion proteins were detected directly by fluorescence microscopy after fixation of cells. The distribution of pVI, iVI and VI 22 h after infection of HeLa cells with Ad2 was detected by immunofluorescence using an antibody to aa 94–170 of pVI (h) after fixation of the cells. Bars, 10 μm.

The different constructs were cleaved with varying efficiency: 20.1 and 20.2 were cleaved poorly, whereas 20.3–20.6 were cleaved more efficiently (results not shown). This was consistent with the observation above that the fusion protein containing the shortest (34 aa) insert from pVI was not localized to the nucleus as efficiently as those with a longer insert, possibly because steric factors hindered access to the relevant sequence motifs.

Table 2. Construction of plasmids expressing fusions of sequences derived from pVI with YFP and CFP

The 2A-CFP-2A region was removed from the original plasmid (construct 20) and replaced with DNA encoding: aa 217–250 from pVI to form construct 20.1; aa 172–250 from pVI to form construct 20.3; and full-length (aa 1–250) pVI to form construct 20.5. The 2A-encoding region at the 3′ end of YFP was removed from construct 20 and replaced with DNA encoding: aa 217–250 from pVI to form construct 20.2; aa 172–250 from pVI to form construct 20.4; and full-length (aa 1–250) pVI to form construct 20.6.

Construct	pVI residues inserted at pVI*	Size of pVI insert (aa)	Construct no.	Localization†
YFP-2A-CFP-2A-pac	–	–	20	C/N
YFP-pVI C*-pac	217–250	34	20.1	N
	172–250	79	20.3	N
	1–250	250	20.5	N
YFP-pVI C*-CFP-2A-pac	217–250	34	20.2	C/N
	172–250	79	20.4	N
	1–250	250	20.6	N

†C, Cytoplasm; N, nucleus.

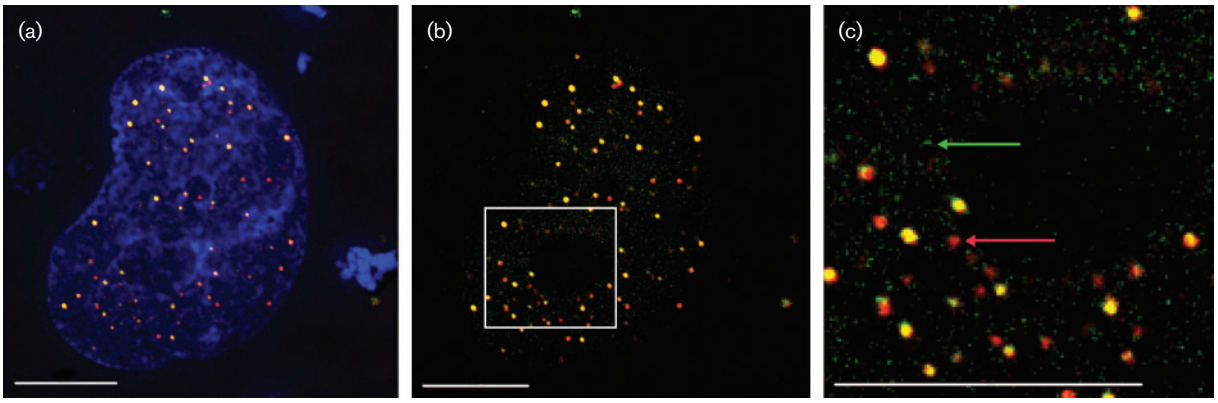

Fig. 6. Cleavage of construct 20.4 during Ad2 infection. HeLa cells were transfected with a plasmid containing construct 20.4 (Table 2) and, 15 h after transfection, were infected with Ad2. After a further 32 h, cells were fixed and examined by fluorescence microscopy with (a) and without (b) DAPI staining. The boxed section in (b) is shown enlarged (c). The intact fusion protein was apparent as yellow speckles and the arrows indicate the presence of separated EYFP and ECFP fusions (appearing red and green, respectively, under the conditions used). Bars, 15 μm.

To test the possibility that the constructs with the larger inserts from pVI could act as markers of adenain activity, HeLa cells were transfected with construct 20.4 and 15 h later infected with Ad2. Fig. 6 shows the pattern of fluorescence 32 h after Ad2 infection. As expected, the intact fusion protein accumulated in the nucleus (Fig. 6a) with the punctate distribution observed previously (Fig. 5). Under the conditions used, the intact fusion proteins displayed a yellow fluorescence (Fig. 5f) and the consequence of protease activity was evident with the appearance of red fluorescence from the separated EYFP fusion and green fluorescence from the pVI-CT–ECFP fusion (Fig. 6b and c). These experiments with fluorescent substrates showed that adenain is proteolytically active in the nucleus approximately 30–32 h after initial infection and that our synthetic fluorescent substrates could be used to assess *in vivo* protease activity at different points during adenoviral infection.

DISCUSSION

The results presented here confirm and extend previous observations (Cabrita *et al.*, 1997) that the first two residues (GV) and last two residues (CF) of pVI-CT play a major role in formation of the catalytically active pVI-CT–adenain heterodimer. Similar conclusions were reached by Baniecki *et al.* (2001) by using a different approach. These authors derived K_d values from the kinetic constants that were obtained from activity assays by using the fluorogenic substrate LRGG-rhodamine (McGrath *et al.*, 1996) in the presence and absence of DNA, reporting that, with wild-type pVI-CT, there was a 50-fold decrease in the binding affinity and a threefold increase in k_{cat} following the inclusion of single-stranded DNA. Not all studies on adenain find that DNA has an influence on its activity (Webster *et al.*, 1994; Diouri *et al.*, 1995), and it has been suggested (McGrath *et al.*, 2001) that the differing substrates used may contribute to this discrepancy. Accordingly, we adopted an approach that did not depend on the use of substrates or the measurement of catalytic activity. This study used the differing mobilities of adenain and the adenain–pVI-CT complex in native gel electrophoresis to provide a more direct measure of the concentrations of bound and free pVI-CT. The binding constants obtained were in accord with those found by Baniecki *et al.* (2001) in the absence of DNA, although generally lower. We also used the method of Baniecki *et al.* (2001) to determine K_d values from activity assays with z-LRGG-AMC as a substrate and found good agreement with the data from the native gel method (Table 1). In accord with our previous observations with other substrates, we found that DNA had no influence on the activity observed when using this substrate (results not shown).

The finding that the KRRR motif was not a major factor in the interaction of pVI-CT and adenain, nor in the development of catalytic activity by the complex, led us to investigate the possibility that it might act as an NLS. The results presented indicate that this sequence is capable of directing proteins whose distribution is normally cytoplasmic to the nucleus, and studies with PK defined the minimum requirement for nuclear accumulation to be the tripeptide KRR. Interestingly, the pattern of localization within the nucleus (a distinctive punctate appearance) was identical to that observed for pVI during adenovirus infection (Table 2), suggesting that the C-terminal region may have further specificity for targeting within the nucleus.

The viral protein pVI, from which pVI-CT was derived, contains two potential NLSs. That found in pVI-CT is close to the C terminus of the 250 aa protein and the other (KRPRP) is close to the centre at aa 131–135. Although the KRRR sequence was sufficient for the nuclear targeting of PK (Fig. 4), EGFP and (provided they were part of a

sufficiently extended linker) combinations of EYFP, ECFP and Pac (Fig. 5) required both the KRPRP and KRRR signals for the nuclear localization of pVI. The inability of iVI(1–239)–EGFP to accumulate in the nucleus in a similar manner to pVI–EGFP supported the general concept that the protease does not cleave pVI-CT until the maturation stage, which takes place following virion assembly in the nucleus.

Wodrich *et al.* (2003) provided evidence that the presence of two NESs, in addition to the two NLSs, allows pVI to shuttle between the nucleus and the cytoplasm, transporting the hexon protein to the nucleus in the process. Our data are in agreement in so far as they suggest the concept of pVI-CT as a nuclear targeting sequence, and these findings provide a rationale for the requirement for both NLSs in the nuclear targeting of pVI. This would suggest that if the ratio of NES to NLS is altered from 2 : 2 to 2 : 1 (as seen with the CM–EGFP and MM–EGFP constructs), the cytoplasmic accumulation of the fusion proteins is promoted. However, the pVI-CT constructs 20.1, 20.3 and 20.4 carried one NLS and one NES, and the finding of nuclear accumulation suggested the predominance of the NLS. In contrast to the results reported by Wodrich *et al.* (2003), we found no evidence of pVI leaving the nucleus following transfection (by using various fluorescent constructs) or following infection of cells with adenovirus (determined by immunofluorescence). In our studies, the distribution of the expressed pVI was consistent in both the transfections and infections.

ACKNOWLEDGEMENTS

We are grateful to P. de Felipe for advice and for the pdf20 plasmid, to W. C. Russell and D. Young for antisera, to P. Talbot for technical support and to T. Vaughan for helpful discussion and advice.

REFERENCES

Anderson, C. W. (1990). The proteinase polypeptide of adenovirus serotype 2 virions. *Virology* **177**, 259–272.

Anderson, C. W., Baum, P. R. & Gesteland, R. F. (1973). Processing of adenovirus 2-induced proteins. *J Virol* **12**, 241–252.

Atherton, E., Cameron, L. R. & Sheppard, R. C. (1988). Peptide synthesis. 10. Use of pentafluorophenyl esters of fluorenyl methoxycarbonylamino acids in solid phase peptide synthesis. *Tetrahedron* **44**, 843–857.

Baniecki, M. L., McGrath, W. J., McWhirter, S. M., Li, C., Toledo, D. L., Pellicena, P., Barnard, D. L., Thorn, K. S. & Mangel, W. F. (2001). Interaction of the human adenovirus proteinase with its 11-amino acid cofactor pVIc. *Biochemistry* **40**, 12349–12356.

Boudin, M.-L., D'Halluin, J.-C., Cousin, C. & Boulanger, P. (1980). Human adenovirus type 2 protein IIIa. II. Maturation and encapsidation. *Virology* **101**, 144–156.

Cabrita, G., Iqbal, M., Reddy, H. & Kemp, G. (1997). Activation of the adenovirus protease requires sequence elements from both ends of the activating peptide. *J Biol Chem* **272**, 5635–5639.

Chen, P. H., Ornelles, D. A. & Shenk, T. (1993). The adenovirus L3 23-kilodalton proteinase cleaves the amino-terminal head domain from cytokeratin 18 and disrupts the cytokeratin network of HeLa cells. *J Virol* **67**, 3507–3514.

Ding, J., McGrath, W. J., Sweet, R. M. & Mangel, W. F. (1996). Crystal structure of the human adenovirus proteinase with its 11 amino acid cofactor. *EMBO J* **15**, 1778–1783.

Diouri, M., Geoghegan, K. F. & Weber, J. M. (1995). Functional characterization of the adenovirus proteinase using fluorogenic substrates. *Protein Pept Lett* **2**, 363–370.

Goldenberg, D. P. (1989). Analysis of protein conformation by gel electrophoresis. In *Protein Structure: A Practical Approach*, pp. 225–250. Edited by T. Creighton. Oxford: IRL Press.

Greber, U. F. (1998). Virus assembly and disassembly: the adenovirus cysteine protease as a trigger factor. *Rev Med Virol* **8**, 213–222.

Grierson, A. W., Nicholson, R., Talbot, P., Webster, A. & Kemp, G. (1994). The protease of adenovirus serotype 2 requires cysteine residues for both activation and catalysis. *J Gen Virol* **75**, 2761–2764.

Hong, J. S. & Engler, J. A. (1991). The amino terminus of the adenovirus fiber protein encodes the nuclear localization signal. *Virology* **185**, 758–767.

Jones, S. J., Iqbal, M., Grierson, A. W. & Kemp, G. (1996). Activation of the protease from human adenovirus type 2 is accompanied by a conformational change that is dependent on cysteine-104. *J Gen Virol* **77**, 1821–1824.

Kalderon, D., Roberts, B. L., Richardson, W. D. & Smith, A. E. (1984). A short amino acid sequence able to specify nuclear location. *Cell* **39**, 499–509.

Lyons, R. H., Ferguson, B. Q. & Rosenberg, M. (1987). Pentapeptide nuclear localization signal in adenovirus E1a. *Mol Cell Biol* **7**, 2451–2456.

Mangel, W. F., McGrath, W. J., Toledo, D. L. & Anderson, C. W. (1993). Viral DNA and a viral peptide can act as cofactors of adenovirus virion proteinase activity. *Nature* **361**, 274–275.

McGrath, W. J., Abola, A. P., Toledo, D. L., Brown, M. T. & Mangel, W. F. (1996). Characterization of human adenovirus proteinase activity in disrupted virus particles. *Virology* **217**, 131–138.

McGrath, W. J., Baniecki, M. L., Li, C., McWhirter, S. M., Brown, M. T., Toledo, D. L. & Mangel, W. F. (2001). Human adenovirus proteinase: DNA binding and stimulation of proteinase activity by DNA. *Biochemistry* **40**, 13237–13245.

Roberts, B. L., Richardson, W. D. & Smith, A. E. (1987). The effect of protein context on nuclear location signal function. *Cell* **50**, 465–475.

Rodriguez, M. S., Dargemont, C. & Hay, R. T. (2001). SUMO-1 conjugation *in vivo* requires both a consensus modification motif and nuclear targeting. *J Biol Chem* **276**, 12654–12659.

Russell, W. C. & Blair, G. E. (1977). Polypeptide phosphorylation in adenovirus-infected cells. *J Gen Virol* **34**, 19–35.

Söling, A., Simm, A. & Rainov, N. G. (2002). Intracellular localization of herpes simplex virus type 1 thymidine kinase fused to different fluorescent proteins depends on choice of fluorescent tag. *FEBS Lett* **527**, 153–158.

Tremblay, M. L., Dery, C. V., Talbot, B. G. & Weber, J. (1983). In vitro cleavage specificity of the adenovirus type 2 proteinase. *Biochim Biophys Acta* **743**, 239–245.

Weber, J. (1976). Genetic analysis of adenovirus type 2. III. Temperature sensitivity of processing viral proteins. *J Virol* **17**, 462–471.

Webster, A., Russell, W. C. & Kemp, G. D. (1989). Characterization of the adenovirus proteinase: development and use of a specific peptide assay. *J Gen Virol* **70**, 3215–3223.

Webster, A., Hay, R. T. & Kemp, G. (1993). The adenovirus protease is activated by a virus-coded disulphide-linked peptide. *Cell* **72**, 97–104.

Webster, A., Leith, I. R. & Hay, R. T. (1994). Activation of adenovirus-coded protease and processing of preterminal protein. *J Virol* **68**, 7292–7300.

Wodrich, H., Guan, T., Cingolani, G., Von Seggern, D., Nemerow, G. & Gerace, L. (2003). Switch from capsid protein import to adenovirus assembly by cleavage of nuclear transport signals. *EMBO J* **22**, 6245–6255.